Thermalization Dynamics of Nonlinear Non-Hermitian Optical Lattices

Georgios G. Pyrialakos,[1,*] Huizhong Ren,[1] Pawel S. Jung,[1,2] Mercedeh Khajavikhan,[1,3] and Demetrios N. Christodoulides[1,†]
[1]CREOL, The College of Optics and Photonics, University of Central Florida, Orlando, Florida 32816, USA
[2]Faculty of Physics, Warsaw University of Technology, 00-662 Warsaw, Poland
[3]Ming Hsieh Department of Electrical and Computer Engineering, University of Southern California, Los Angeles, California 90089, USA

(Received 1 February 2022; revised 5 April 2022; accepted 2 May 2022; published 23 May 2022)

We develop a rigorous theoretical framework based on principles from statistical mechanics that allows one to predict the equilibrium response of classical non-Hermitian arrangements in the weakly nonlinear regime. In this respect, we demonstrate that a pseudo-Hermitian configuration can always be driven into thermal equilibrium when a proper nonlinear operator is paired with the linear Hamiltonian of the system. We show that, in this case, the system will thermodynamically settle into an irregular pattern that does not resemble any known statistical distribution. Interestingly, this stable equilibrium response is associated with a Rayleigh-Jeans law when viewed within an appropriately transformed space that displays unitary dynamics. By considering a non-Hermitian Su-Schrieffer-Heeger chain, our results indicate that the thermodynamic equilibrium will always favor the edge modes instead of the ground state, in stark contrast to conventional nonlinear Hermitian configurations. Moreover, non-Hermitian lattices are shown to exhibit unusually high heat capacities, potentially acting as optical heat reservoirs to other Hermitian systems, by employing only a small number of sites and low power levels.

DOI: 10.1103/PhysRevLett.128.213901

In the last decade, optics has witnessed a renewal of interest in non-Hermitian settings with the advent of now highly adopted concepts emerging from theories like parity-time (PT) symmetry [1,2]. This led to a theoretical and experimental burst of activities that unraveled a host of novel phenomena that have no counterpart in Hermitian environments [3–13]. These include, for example, the demonstration of the non-Hermitian skin effect, a process that can arise due to the unique topological structure associated with non-Hermiticity [14–25]. In recent years, substantial effort has been devoted to pseudo-Hermitian arrangements that can always be associated with non-Hermitian Hamiltonians exhibiting completely real eigenspectra [26,27]. These configurations are endowed with a richer set of properties, stemming from their ability to form exceptional points in their parameter space [28–33]. The unique set of attributes associated with pseudo-Hermiticity have been explored in a variety of photonic settings [34–36].

The interplay between nonlinearity and non-Hermiticity can lead to a wealth of novel optical phenomena in a variety of photonic settings. Over the years, it has been systematically explored, mainly within the context of optical solitons [37–39], in various amplifying systems governed by Ginzburg-Landau equations as well as in pseudo-Hermitian arrangements [40–48]. Meanwhile, a regime that to this day remains largely unexplored emerges when considering multimode non-Hermitian configurations under weak nonlinear conditions, where intricate wave-mixing processes are at play. In these settings, the analysis of their dynamic response presents an utterly complex problem, especially when hundreds or even thousands of modes are involved. Consequently, the only pragmatic approach to decipher the behavior of these configurations is by deploying notions from thermodynamics and statistical mechanics [49]. To this end, many challenges still remain, given that the integrals of motion, a necessary ingredient for the development of a thermodynamic theory [49–52], do not always manifest themselves. Moreover, even pseudo-Hermitian configurations can exhibit extreme instabilities under nonlinear conditions that may result in an exponential growth of power and consequently the absence of an equilibrium response [53,54].

To address these issues, in this Letter we pursue a dual objective: (i) the classification of non-Hermitian systems that can display thermalization, and (ii) the development of a consistent theoretical framework for predicting their modal occupancy distribution at equilibrium. Here, the first objective will be carried out by developing a universal set of rules that will dictate whether a classical non-Hermitian system can be driven into thermal equilibrium. In this respect, we focus on arrangements that can self-thermalize in isolation, as opposed to open systems that are coupled to a heat bath. Although, in principle, a non-Hermitian system cannot be isolated due to gain and dissipation effects, the intrinsic invariants that can manifest themselves in these arrangements will be proven sufficient in describing the thermalization process.

In developing an optical thermodynamic theory for nonlinear optical configurations, one must first define two invariants of motion. In Hermitian systems, these can be expressed using the projected amplitudes c_n on the linear eigenbasis as

$$P = \sum_n |c_n|^2, \qquad U = -\sum_n \varepsilon_n |c_n|^2, \tag{1}$$

where n is the eigenmode index, ε_n represent the eigenvalues of the linear spectrum, P is the total physical power, and U corresponds to the linear part of the total Hamiltonian $H_T = U + H_{\mathrm{NL}}$ (the nonlinear component H_{NL} is omitted in the weakly nonlinear regime). The invariance requirement for P restricts the development of such a thermodynamic theory only to conservative and in extension fully Hermitian models. Therefore, for non-Hermitian systems, one must identify new integrals of motion. Such invariants are manifested in pseudo-Hermitian arrangements due to their association with a representation that displays unitary dynamics, a property that is absent in structures with complex spectra.

We begin our analysis by first defining a generic pseudo-Hermitian nonlinear system with a real eigenspectrum $\{\epsilon_n\}$ described by the following equation:

$$i\frac{da_i}{dt} = H^{\mathrm{L}}_{ij} a_j + H^{\mathrm{NL}}_{ij} a_j, \tag{2}$$

where the linear non-Hermitian Hamiltonian H^{L} is accompanied by the nonlinear operator H^{NL}. This operator can be, for example, Kerr nonlinear $\gamma|a_i|^2$ where, γ is normalized to unity. Here, the system will be operated in the weakly nonlinear regime by appropriately controlling the magnitude of the total optical power (P). The linear Hamiltonian H^{L} in Eq. (1) is associated with a biorthogonal basis $|v\rangle$ that acts as a reciprocal space to the nonorthogonal eigenmode basis $|u\rangle$.

We analyze this configuration by adopting a similarity transformation Q (i.e., $Q(H^{\mathrm{L}} + H^{\mathrm{NL}})Q^{-1}$) that renders the linear part of the Hamiltonian $H'^{\mathrm{L}} = QH^{\mathrm{L}}Q^{-1}$ into a fully Hermitian operator. Such a transformation can always be found for pseudo-Hermitian arrangements (such as a PT-symmetric system in the unbroken phase), thus providing an equivalent conservative representation that displays an identical spectrum with the original non-Hermitian Hamiltonian [26,27]. This property allows one to monitor the underpinning dynamics in a Hermitian environment where linear integrals of motion exist.

To observe thermalization in pseudo-Hermitian arrangements one must first impose two additional necessary conditions, beyond the emergence of the linear invariants. The first is the presence of a physical mechanism that can initiate the ergodic multiwave mixing process. Here, this role is undertaken by the nonlinear operator H^{NL}, which can lead to chaotic evolution and hence thermalization—a process that is enabled irrespective of the operator's particular structure. The second condition entails that the linear invariants must persist after engaging H^{NL} in Eq. (2). For this to be true, the nonlinear part of the transformation, $H'^{\mathrm{NL}} = QH^{\mathrm{NL}}Q^{-1}$ must also correspond to a Hermitian operator. Otherwise, one cannot establish a proper representation associated with a unitary evolution under nonlinear conditions and the linear conserved quantities will no longer manifest themselves.

To verify the validity of these claims, we begin by examining two particular systems with a Kerr-type nonlinearity: a PT-symmetric one-dimensional chain of optical elements and a non-Hermitian Su-Schrieffer-Heeger (SSH) model with asymmetric couplings between nearest neighbors (the real-space Hamiltonians are given in Note II of the Supplemental Material [55]). A Kerr nonlinearity corresponds to a Hermitian nonlinear operator with diagonal elements given by $|a_i|^2$ (before the transformation is applied). A sufficient condition for preserving the Hermiticity of $QH^{\mathrm{NL}}Q^{-1}$ is for Q to be an orthogonal matrix ($Q^TQ = QQ^T = I$). However, not both pseudo-Hermitian systems can transform under an orthogonal matrix, a property that, as we will see, restricts which of the two configurations can exhibit thermalization.

In order to identify the presence of an equilibrium response, it is necessary to analyze the time evolution of various relevant quantities. In Fig. 1, we plot the time dynamics of four quantities by exciting simultaneously 10 out of the 21 linear lattice modes (supermodes) in a lattice with $N = 21$ sites. These four quantities correspond to the physical power P, the effective internal energy U, the pseudo power P_s, and the pseudo energy U_s. These two pairs are defined according to Eq. (1) within the non-Hermitian and Hermitian representation, respectively. In particular the two Hermitian quantities can be expressed according to Eq. (1) by $P_s = \sum_n |c'_n|^2$ and $U_s = \sum_n \varepsilon_n |c_{n'}|^2$ via the Hermitian projected amplitudes c'_n.

In the linear regime of Fig. 1(a), the physical power P oscillates in both systems, an expected consequence of pseudo-Hermiticity, while the transformed power P_s remains constant as imposed by the underlying unitary evolution of the Hermitian representation. This picture changes when the Kerr operator is involved. In this case, the PT-symmetric system oscillates in both the physical and transformed representation while exponentially gaining power as time progresses. On the other hand, the dynamic evolution of the SSH non-Hermitian chain remains stable for arbitrarily large times. These two different outcomes are directly correlated to the properties of the transformation matrix Q. In the case of the SSH chain, Q is an orthogonal matrix (and in particular diagonal), in agreement with the requirement imposed previously. The stability of the nonlinear SSH chain leads to a well-defined equilibrium state for the average modal occupancy strengths as shown in Fig. 1(d), for a lattice of $N = 21$ sites. However, the

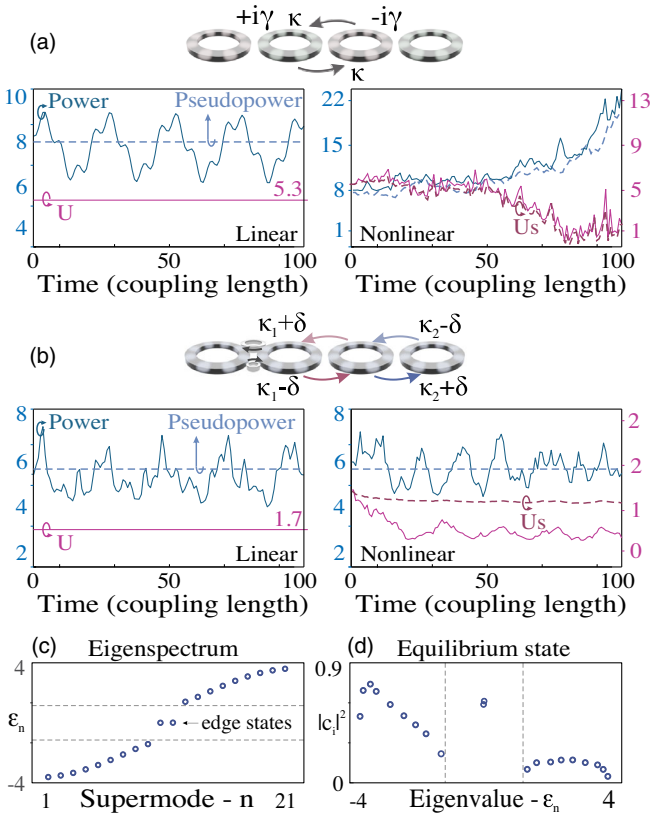

FIG. 1. (a) A PT-symmetric configuration of optical cavities with alternating gain and loss ($\kappa = 1$, $\gamma = 0.1$). During linear evolution, the physical power oscillates and the pseudo power now assumes the role of the invariant of motion. During nonlinear evolution, no invariant can be identified and power is expected to grow indefinitely. The time in figures is measured in inverse coupling units. (b) An arrangement of optical cavities with asymmetric couplings ($\kappa_1 = 1$, $\kappa_2 = 2$, $\delta = 0.2$). Two invariants of motion (P_s and U_s) are now present in both the linear and nonlinear regime. (c) The linear eigenspectrum of the system in (b). (d) The average power occupancies of the same system settle into a stable equilibrium state in the original supermode basis.

distribution is not associated with any familiar form (for example with the Rayleigh-Jeans distribution encountered in optics [56]) and requires further investigation.

In what follows, we focus our study on arrangements with anisotropic couplings due to the instability exhibited by PT-symmetric systems that forbids thermalization under Kerr-type nonlinearities. Nonetheless, the formalism that will be laid herein will be applicable to any pseudo-Hermitian configuration if one finds a proper nonlinear operator that preserves Hermiticity under a similarity transformation Q. In this respect, in Note IV of the Supplemental Material [55], we outline a strategy that allows one to properly identify such a nonlinear operator and we showcase the emergence of thermalization and a stable equilibrium response for the PT-symmetric chain of Fig. 1(a). Therefore, we prove, in principle, that any classical pseudo-Hermitian system can thermalize.

Having identified two integrals of motion we now seek to derive an equilibrium distribution for the linear modal amplitudes $|c_n|^2$. To this end, we begin in the Hermitian representation and maximize the optical entropy defined by $S = \sum \ln |c'_n|^2$ subjected to the two constrains via the use of Lagrange multipliers (see Note I in the Supplemental Material [55]). This process results in a Rayleigh-Jeans law for the average Hermitian modal amplitudes $|c'_n|$, given by

$$\langle |c'_n|^2 \rangle = -T/(\varepsilon_n + \mu), \tag{3}$$

where the two intensive variables T and μ correspond to an effective optical temperature and optical chemical potential associated with U_s and P_s respectively.

To derive an equilibrium distribution in the original eigenbasis, we must first apply a reverse transformation on the amplitudes $|c_n|$. The modal occupancies between the two representations are directly related via a matrix operator, $c_n = \sum_m A_{nm} c'_m = \sum_m \langle v_n | Q^{-1} | u_m \rangle c'_m$. However, the distribution given by Eq. (3) corresponds to a statistical average and therefore cannot be treated directly in this form due to emergent correlations between the modes. Nonetheless, considering that a similarity transformation preserves the eigenstructure of H^{L}, the operator A reduces always into a purely diagonal matrix ($A_{nm} = 0$, $A_{nn} \equiv A_n \neq 0$). In this respect, a direct transformation of Eq. (3) can be performed, resulting in a weighted Rayleigh-Jeans law:

$$\langle |c_n|^2 \rangle = -(1/A_n^2) T/(\varepsilon_n + \mu). \tag{4}$$

This equation provides a direct prediction of the average modal occupancies for a pseudo-Hermitian system in the weakly nonlinear regime, as expressed in the original eigenbase. Likewise, the two integrals of motion can be transformed to the original eigenbasis, acquiring the following forms:

$$P_s = \sum_n A_n^2 |c_n|^2, \qquad U_s = -\sum_n A_n^2 \varepsilon_n |c_n|^2. \tag{5}$$

The intensive variables T and μ can be calculated by combining Eqs. (4) and (5) and the universal equation of state that is given by $U_s - \mu P_s = MT$, with M representing the total number of lattice supermodes. In this respect, one can always predict the equilibrium Rayleigh-Jeans distribution for any initial excitation.

To validate this theoretical framework, we rely on numerical simulations in the SSH non-Hermitian optical chain of Fig. 1(b). The lattice comprises a total of $N = 21$ sites with $\kappa_1 = 1$, $\kappa_2 = 2$, $\delta = 0.4$ and is truncated appropriately so that a pair of topological edge states emerges at zero energy. In order to observe an equilibrium state, we obtain the modal occupancies by averaging over 200 individual ensembles. Each ensemble corresponds to a

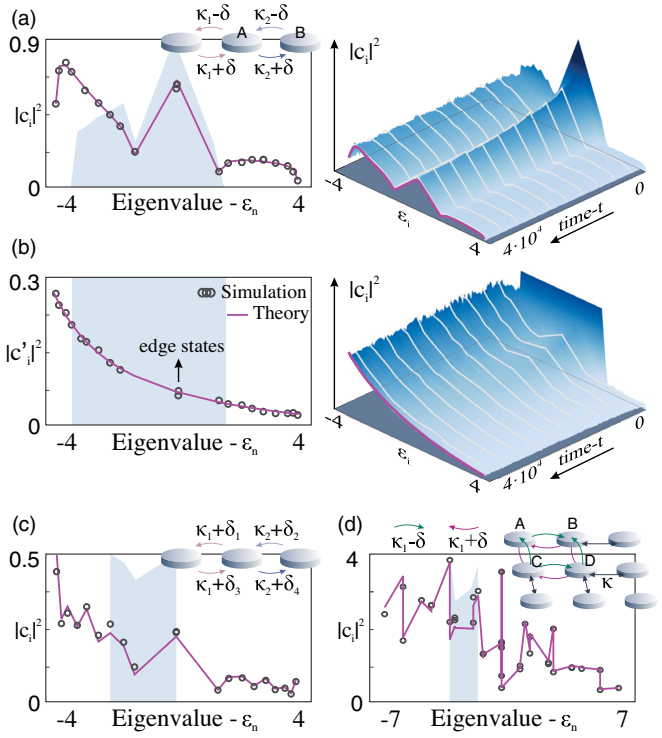

FIG. 2. (a) A nonlinear non-Hermitian SSH chain with $\kappa_1 = 1$, $\kappa_2 = 2$, and $\delta = 0.2$ reaches equilibrium in the original linear modal basis that matches a weighted Rayleigh-Jeans distribution. (b) The $|c'_n|^2$ magnitudes in the Hermitian representation settle into a regular Rayleigh-Jeans distribution. The blue shaded areas denote the initial distribution, which is chosen to be uniform in the Hermitian-projected space. (c) Equilibrium state of the SSH chain with $\kappa_1 = 1$, $\kappa_2 = 2$ and random δ_n terms sampled uniformly from [0, 1] (d) The modal occupancies are precisely predicted for a 2D lattice with anisotropic couplings ($\kappa_1 = 1$, $\kappa_2 = 2$, $\kappa = 1$, and $\delta = 0.5$) employing 3 unit cells (36 sites) through the corresponding Hermitian lattice.

separate simulation run, initiated by a light excitation that uniformly populates a continuous set of supermodes within the Hermitian representation (in this example, all modes with eigenvalues in the range $-4 < \epsilon_n < 1$) albeit with random phases. This enforces the same values for the two invariants [U_s and P_s of Eq. (5)] for each simulation run. Alternatively, an equivalent result can be extracted via a single simulation run, by averaging or sampling on the time axis, a direct manifestation of ergodicity.

Figure 2(a) illustrates a comparison between the theoretically predicted and simulated averages of the linear modal amplitudes at equilibrium for an initial state with $P_s = 6$ and $U_s = -2$. The projected amplitudes within the linear mode basis are properly normalized at unity ($\langle v_n|u_n\rangle = 1$ and $\langle u_n|u_n\rangle = 1$). After a sufficiently long evolution time, the numerical results relax into the weighted Rayleigh-Jeans distribution of Eq. (4). In this particular example, the weights $1/A_9^2$, $1/A_{10}^2$ that correspond to the two topological edge states acquire higher values in relation to the bulk modes and as a result the edge modes accumulate more power at equilibrium. This is in stark contrast to conventional Hermitian systems where at thermal equilibrium the fundamental (ground state) or highest order mode is always favored for negative and positive temperatures, respectively. Moreover, in Fig. 2(b) we observe the evolution in the transformed representation and verify the equilibrium response fully agrees with the Rayleigh-Jeans law given by Eq. (3).

We next proceed to study a number of more intricate examples.A straightforward extension of the simple non-Hermitian SSH chain can be established by including random anisotropy terms δ_n. Figure 2(c) verifies the correspondence between the theoretically predicted and simulated outcome at equilibrium, considering a lattice excitation with $P_s = 6$ and $U_s = -1$. Because of the randomness of δ_n on the spatial axis, the weights A_n of Eq. (4) become irregular, resulting in a Rayleigh-Jeans-like curve with strong noise. Nonetheless, the prediction remains highly accurate. Next, we consider a two-dimensional non-Hermitian lattice that can exhibit a higher-order non-Hermitian skin effect [57]. We simulate a highly anisotropic case with coupling parameters $(\kappa_1 = 1, \delta = 2, \kappa = 1)$ and extract the equilibrium distribution of power among the linear modes of the system. The continuous curve of Fig. 2(d) corresponds to the theoretically predicted distribution and provides once again an accurate estimate.

The previous examples showcased that a prediction of the equilibrium response is attainable with high accuracy but did not yet reveal the true nature of the intensive variables T and μ. To provide further insight into this aspect, we explore multilattice interactions, i.e., cases where two or more lattices are allowed to optically interact and therefore exchange optical energies U_s. In Hermitian systems, this process causes a relaxation to a common final temperature in both lattices, an outcome consistent with classical thermodynamics. In this respect we introduce an additional nonlinear operator H^{CP} to Eq. (2) that couples two oppositely polarized lattices (with state vectors a_n and b_n) via cross-phase terms ($H_a^{\mathrm{CP}} = |a_n|^2 b_n$, $H_b^{\mathrm{CP}} = |b_n|^2 a_n$) (see Note V in the Supplemental Material [55]). The matrices H^{CP} and H^{NL} are both diagonal, which simultaneously guarantees the Hermiticity of both the transformed nonlinear $QH^{\mathrm{NL}}Q^{-1}$ and cross-phase $QH^{\mathrm{CP}}Q^{-1}$ operators.

In the example of Fig. 3, we illustrate a comparison between two cases: a Hermitian-to-Hermitian and a non-Hermitian-to-Hermitian square lattice pairing. In either case, both lattices comprise a total of 50 elements and interact on the first and last row of sites that they share in common. We excite all four lattices with the same physical power $P = 0.5$ and different U_s corresponding to distinct optical temperatures. Figures 3(c) and 3(d) display the temperature variation over a long period of time until a common value is attained. In the non-Hermitian-to-Hermitian pairing, the final value for T ends up much closer

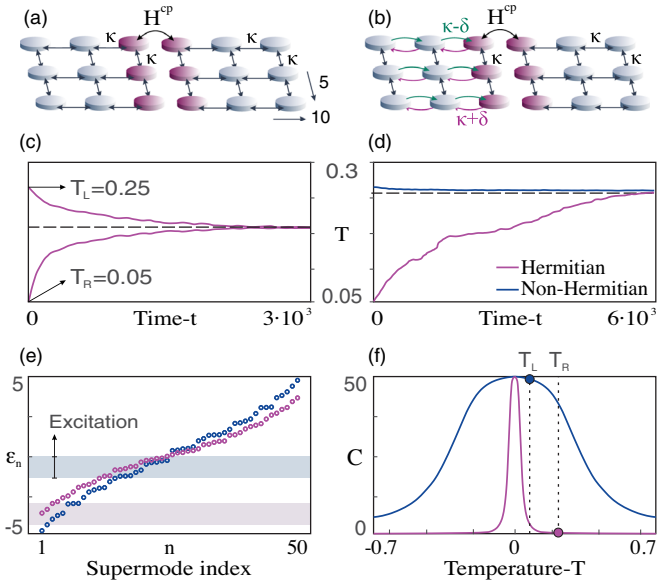

FIG. 3. (a) Two Hermitian square lattices with $\kappa = 1$ are excited with oppositely polarized light, sharing the column of elements shaded in red. The cross-phase modulation operator H^{CP} allows exchange of optical internal energy between the two arrangements. (b) A non-Hermitian lattice with $\kappa = 1$ and $\delta = 0.5$ is paired to a Hermitian lattice with $\kappa = 2$. (c) The lattices of (a), excited with power $P = 0.5$ ($P_s = 0.5$) at different temperatures T_{Left} and T_{Right} eventually reach a common temperature $T = 0.18$. (d) The non-Hermitian lattice of (b) acts as a heat bath to its Hermitian counterpart. Both are excited with $P = 0.5$ ($P_s = 6$ and $P_s = 0.5$ for the two lattices, respectively). (e) The eigenmodes of the two lattices in (b) sorted by their eigenvalues. The shaded regions indicate the excitation used in (d). (f) Heat Capacity $C = \partial U_s/\partial T$ of the two lattices in (b).

to the non-Hermitian system's original value. This effect is directly correlated to an unusually large optical heat capacity exhibited by the non-Hermitian system (defined by $C = \partial U_s/\partial T$), a measure that demonstrates the amount of internal energy exchange required for an infinitesimal variation of temperature. Figure 3(f) displays the heat capacity of the two lattices, over the temperature range $[-0.7, 0.7]$, revealing a large difference in magnitude between the two curves, an indication that a similar variation in temperature requires a much larger change for U_s in the non-Hermitian lattice. Essentially, a non-Hermitian system can potentially act as an optical heat reservoir to a secondary optical system by employing the same number of sites but a much lower power level to an equivalent all-Hermitian heat bath configuration.

In this Letter, we developed a theoretical framework capable of describing thermalization dynamics over a broad range of nonlinear non-Hermitian systems with on-site nonlinearities. Within this context, one may explore different non-Kerr or even nonlocal nonlinear operators H^{NL} that may allow thermalization in a wider class of pseudo-Hermitian configurations.

This work was partially supported by ONR MURI (N00014-20-1-2789), AFOSR MURI (FA9550-20-1-0322, FA9550-21-1-0202), National Science Foundation (NSF) (DMR-1420620, EECS-1711230,ECCS CBET 1805200, ECCS 2000538, ECCS 2011171), MPS Simons collaboration (Simons Grant No. 733682), W. M. Keck Foundation, USIsrael Binational Science Foundation (BSF: 2016381), US Air Force Research Laboratory (FA86511820019), DARPA (D18AP00058), Office of Naval Research (N00014-19-1-2052, N00014-20-1-2522), Army Research Office (W911NF-17-1-0481), the Polish Ministry of Science and Higher Education (1654/MOB/V/2017/0), and the Qatar National Research Fund (Grant No. NPRP13S0121-200126). G. G. P. would like to acknowledge the support of the Bodossaki Foundation.

*Corresponding author.
pyrialak@knights.ucf.edu
†Corresponding author.
demetri@creol.ucf.edu

[1] C. M. Bender and S. Boettcher, Real Spectra in Non-Hermitian Hamiltonians Having PT Symmetry, Phys. Rev. Lett. **80**, 5243 (1998).
[2] C. M. Bender, M. V. Berry, and A. Mandilara, Generalized PT symmetry and real spectra, J. Phys. A **35**, 192 (1998).
[3] C. E. Rüter, K. G. Makris, R. El-Ganainy, D. N. Christodoulides, M. Segev, and D. Kip, Observation of parity time symmetry in optics, Nat. Phys. **6**, 192 (2010).
[4] M. Kremer, T. Biesenthal, L. J. Maczewsky, M. Heinrich, R. Thomale, and A. Szameit, Demonstration of a two-dimensional PT-symmetric crystal, Nat. Commun. **10**, 435 (2019).
[5] M. Chitsazi, H. Li, F. Ellis, and T. Kottos, Experimental Realization of Floquet PT-Symmetric Systems, Phys. Rev. Lett. **119**, 093901 (2017).
[6] S. Longhi, Optical Realization of Relativistic Non-Hermitian Quantum Mechanics, Phys. Rev. Lett. **105**, 013903 (2010).
[7] R. El-Ganainy, K. G. Makris, M. Khajavikhan, Z. H. Musslimani, S. Rotter, and D. N. Christodoulides, Non-hermitian physics and PT symmetry, Nat. Phys. **14**, 11 (2018).
[8] Z. Gong, Y. Ashida, K. Kawabata, K. Takasan, S. Higashikawa, and M. Ueda, Topological Phases of Non-Hermitian Systems, Phys. Rev. X **8**, 031079 (2018).
[9] A. F. Tzortzakakis, K. G. Makris, A. Szameit, and E. N. Economou, Transport and spectral features in non-hermitian open systems, Phys. Rev. Research **3**, 013208 (2021).
[10] S. Weidemann, M. Kremer, S. Longhi, and A. Szameit, Non-hermitian anderson transport, arXiv:2007.00294.
[11] S. Weimann, M. Kremer, Y. Plotnik, Y. Lumer, S. Nolte, K. G. Makris, M. Segev, M. C. Rechtsman, and A. Szameit, Topologically protected bound states in photonic parity–time-symmetric crystals, Nat. Mater. **16**, 433 (2017).
[12] I. Komis, S. Sardelis, Z. H. Musslimani, and K. G. Makris, Equal-intensity waves in non-hermitian media, Phys. Rev. E **102**, 032203 (2020).

[13] S. Klaiman, U. Günther, and N. Moiseyev, Visualization of Branch Points inPT-Symmetric Waveguides, Phys. Rev. Lett. **101**, 080402 (2008).
[14] S. Yao and Z. Wang, Edge States and Topological Invariants of Non-Hermitian Systems, Phys. Rev. Lett. **121**, 086803 (2018).
[15] C. H. Lee and R. Thomale, Anatomy of skin modes and topology in non-hermitian systems, Phys. Rev. B **99**, 201103 (2019).
[16] S. Longhi, Probing non-hermitian skin effect and non-bloch phase transitions, Phys. Rev. Research **1**, 023013 (2019).
[17] T. Helbig, T. Hofmann, S. Imhof, M. Abdelghany, T. Kiessling, L. W. Molenkamp, C. H. Lee, A. Szameit, M. Greiter, and R. Thomale, Generalized bulk–boundary correspondence in non-hermitian topolectrical circuits, Nat. Phys. **16**, 747 (2020).
[18] K. Yokomizo and S. Murakami, Non-Bloch Band Theory of Non-Hermitian Systems, Phys. Rev. Lett. **123**, 066404 (2019).
[19] K. Zhang, Z. Yang, and C. Fang, Correspondence between Winding Numbers and Skin Modes in Non-Hermitian Systems, Phys. Rev. Lett. **125**, 126402 (2020).
[20] S. Weidemann, M. Kremer, T. Helbig, T. Hofmann, A. Stegmaier, M. Greiter, R. Thomale, and A. Szameit, Topological funneling of light, Science **368**, 311 (2020).
[21] D. S. Borgnia, A. J. Kruchkov, and R.-J. Slager, Non-Hermitian Boundary Modes and Topology, Phys. Rev. Lett. **124**, 056802 (2020).
[22] N. Okuma, K. Kawabata, K. Shiozaki, and M. Sato, Topological Origin of Non-Hermitian Skin Effects, Phys. Rev. Lett. **124**, 086801 (2020).
[23] H. Shen, B. Zhen, and L. Fu, Topological Band Theory for Non-Hermitian Hamiltonians, Phys. Rev. Lett. **120**, 146402 (2018).
[24] K. Wang, A. Dutt, C. C. Wojcik, and S. Fan, Topological complex-energy braiding of non-hermitian bands, Nature (London) **598**, 59 (2021).
[25] F. Song, S. Yao, and Z. Wang, Non-Hermitian Topological Invariants in Real Space, Phys. Rev. Lett. **123**, 246801 (2019).
[26] A. Mostafazadeh, Pseudo-hermitian representation of quantum mechanics, Int. J. Geom. Methods Mod. Phys. **07**, 1191 (2010).
[27] A. Mostafazadeh, Pseudo-hermiticity versus PT symmetry: The necessary condition for the reality of the spectrum of a non-hermitian hamiltonian, J. Math. Phys. (N.Y.) **43**, 205 (2002).
[28] B. Zhen, C. W. Hsu, Y. Igarashi, L. Lu, I. Kaminer, A. Pick, S.-L. Chua, J. D. Joannopoulos, and M. Soljačić, Spawning rings of exceptional points out of dirac cones, Nature (London) **525**, 354 (2015).
[29] H. Zhou, C. Peng, Y. Yoon, C. W. Hsu, K. A. Nelson, L. Fu, J. D. Joannopoulos, M. Soljačić, and B. Zhen, Observation of bulk fermi arc and polarization half charge from paired exceptional points, Science **359**, 1009 (2018).
[30] S. Soleymani, Q. Zhong, M. Mokim, S. Rotter, R. El-Ganainy, and S. K. Ozdemir, Chiral coherent perfect absorption on exceptional surfaces, Nat. Commun. **13**, 599 (2022).
[31] A. Hashemi, S. M. Rezaei, S. K. Özdemir, and R. El-Ganainy, New perspective on chiral exceptional points with application to discrete photonics, APL Photonics **6**, 040803 (2021).
[32] Q. Zhong, J. Kou, Ş. Özdemir, and R. El-Ganainy, Hierarchical Construction of Higher-Order Exceptional Points, Phys. Rev. Lett. **125**, 203602 (2020).
[33] A. Roy, S. Jahani, Q. Guo, A. Dutt, S. Fan, M.-A. Miri, and A. Marandi, Nondissipative non-hermitian dynamics and exceptional points in coupled optical parametric oscillators, Optica **8**, 415 (2021).
[34] M. P. Hokmabadi, A. Schumer, D. N. Christodoulides, and M. Khajavikhan, Non-hermitian ring laser gyroscopes with enhanced sagnac sensitivity, Nature (London) **576**, 70 (2019).
[35] Y. Shin, H. Kwak, S. Moon, S.-B. Lee, J. Yang, and K. An, Observation of an exceptional point in a two-dimensional ultrasonic cavity of concentric circular shells, Sci. Rep. **6**, 38826 (2016).
[36] J. Doppler, A. A. Mailybaev, J. Böhm, U. Kuhl, A. Girschik, F. Libisch, T. J. Milburn, P. Rabl, N. Moiseyev, and S. Rotter, Dynamically encircling an exceptional point for asymmetric mode switching, Nature (London) **537**, 76 (2016).
[37] Z. H. Musslimani, K. G. Makris, R. El-Ganainy, and D. N. Christodoulides, Optical Solitons in PT Periodic Potentials, Phys. Rev. Lett. **100**, 030402 (2008).
[38] M. Wimmer, A. Regensburger, M.-A. Miri, C. Bersch, D. N. Christodoulides, and U. Peschel, Observation of optical solitons in PT-symmetric lattices, Nat. Commun. **6**, 7782 (2015).
[39] S. Nixon, L. Ge, and J. Yang, Stability analysis for solitons in PT-symmetric optical lattices, Phys. Rev. A **85**, 023822 (2012).
[40] N. K. Efremidis and D. N. Christodoulides, Discrete Ginzburg-Landau solitons, Phys. Rev. E **67**, 026606 (2003).
[41] L. Ge and R. El-Ganainy, Nonlinear modal interactions in parity-time PT-symmetric lasers, Sci. Rep. **6**, 24889 (2016).
[42] F. Wise, A. Chong, and W. Renninger, High-energy femtosecond fiber lasers based on pulse propagation at normal dispersion, Laser Photonics Rev. **2**, 58 (2008).
[43] J. Yang, Necessity of PT symmetry for soliton families in one-dimensional complex potentials, Phys. Lett. A **378**, 367 (2014).
[44] N. PernetArx *et al.*, Topological gap solitons in a 1d non-hermitian lattice, arXiv:2101.01038.
[45] D. H. Jeon, M. Reisner, F. Mortessagne, T. Kottos, and U. Kuhl, Non-Hermitian CT-Symmetric Spectral Protection of Nonlinear Defect Modes, Phys. Rev. Lett. **125**, 113901 (2020).
[46] R. El-Ganainy, J. I. Dadap, and R. M. Osgood, Optical parametric amplification via non-hermitian phase matching, Opt. Lett. **40**, 5086 (2015).
[47] M. J. Ablowitz and Z. H. Musslimani, Integrable Nonlocal Nonlinear Schrödinger Equation, Phys. Rev. Lett. **110**, 064105 (2013).
[48] M. J. Ablowitz and Z. H. Musslimani, Inverse scattering transform for the integrable nonlocal nonlinear schrödinger equation, Nonlinearity **29**, 915 (2016).
[49] F. O. Wu, A. U. Hassan, and D. N. Christodoulides, Thermodynamic theory of highly multimoded nonlinear optical systems, Nat. Photonics **13**, 776 (2019).

[50] K. G. Makris, F. O. Wu, P. S. Jung, and D. N. Christodoulides, Statistical mechanics of weakly nonlinear optical multimode gases, Opt. Lett. **45**, 1651 (2020).

[51] A. Ramos, L. Fernández-Alcázar, T. Kottos, and B. Shapiro, Optical Phase Transitions in Photonic Networks: A Spin-System Formulation, Phys. Rev. X **10**, 031024 (2020).

[52] N. K. Efremidis and D. N. Christodoulides, Fundamental entropic processes in the theory of optical thermodynamics, Phys. Rev. A **103**, 043517 (2021).

[53] K. Li and P. G. Kevrekidis, PT-symmetric oligomers: Analytical solutions, linear stability, and nonlinear dynamics, Phys. Rev. E **83**, 066608 (2011).

[54] S. Nixon, L. Ge, and J. Yang, Stability analysis for solitons in PT-symmetric optical lattices, Phys. Rev. A **85**, 023822 (2012).

[55] See Supplemental Material at http://link.aps.org/supplemental/10.1103/PhysRevLett.128.213901 for an analytic derivation of the Rayleigh-Jeans law and the equation of state in the Hermitian representation, a methodology for synthesizing a proper nonlinear operator that can thermalize a PT-symmetric Hamiltonian, and a discussion on temperature variations through cross phase interactions.

[56] Z. Eslami, L. Salmela, A. Filipkowski, D. Pysz, M. Klimczak, R. Buczynski, J. M. Dudley, and G. Genty, Two octave supercontinuum generation in a non-silica graded-index multimode fiber, arXiv:2108.09189.

[57] X. Zhang, Y. Tian, J.-H. Jiang, M.-H. Lu, and Y.-F. Chen, Observation of higher-order non-hermitian skin effect, Nat. Commun. **12**, 5377 (2021).